

Anti-TNFA (TNF- α) Treatment Abrogates Radiation-Induced Changes in Vascular Density and Tissue Oxygenation

Ramin Ansari,^a M. Waleed Gaber,^c Bin Wang,^a Christopher B. Pattillo,^a Curtis Miyamoto^b and Mohammad F. Kiani^{a,b,1}

^a Departments of Mechanical Engineering and ^b Radiation Oncology, Temple University, Philadelphia, Pennsylvania; and
^c Department of Biomedical Engineering and Imaging, University of Tennessee Health Science Center, Memphis, Tennessee

Ansari, R., Gaber, M. W., Wang, B., Pattillo, C. B., Miyamoto, C. and Kiani, M. F. Anti-TNFA (TNF- α) Treatment Abrogates Radiation-Induced Changes in Vascular Density and Tissue Oxygenation. *Radiat. Res.* 167, 80–86 (2007).

Ionizing radiation significantly alters the structure and function of microvasculature, which regulates delivery of oxygen to brain tissue. Previous experimental and modeling studies have shown that tissue oxygenation patterns are significantly different in irradiated normal tissue compared to age-matched controls, and the differences are apparent as early as 3 days postirradiation. However, oxygen delivery to irradiated tissue recovers within 6 months postirradiation. Changes in perfusion and oxygenation were studied in a bilaterally (both cerebral hemispheres) and unilaterally (only one hemisphere) irradiated mouse brain model at 6 and 24 h as well as 3, 7, 30, 60 and 120 days postirradiation. The results indicate that significant changes in the number of perfused vessels (as measured by fluorescent DiOC₇ staining) and anatomical vessels (as indicated by CD31 immunohistochemical staining) and tissue oxygenation (by immunohistochemical detection of a fluorescently conjugated monoclonal antibody to EF5) are most pronounced at 3 days postirradiation, while a degree of recovery is observed at later times. However, in the unilaterally irradiated animals, both irradiated and unirradiated (out-of-field) cerebral hemispheres showed similarly significant changes in oxygenation and/or perfusion compared to unirradiated controls. Anti-TNFA treatment inhibited radiation-induced local as well as abscopal effects in the brain tissue. © 2007 by Radiation Research Society

INTRODUCTION

Although glial progenitor cells are radiosensitive, recent studies have suggested that radiation-induced apoptosis of the endothelial cells initiates a cascade of events resulting in injury to various tissues, including the central nervous system (1–3). Therapeutic doses of ionizing radiation have been shown to cause changes in the microvascular network's structure and function (1, 4–6) and regulatory mech-

anisms (7). These changes in turn may cause a reduction in blood flow to the affected tissue, resulting in a lack of oxygen and nutrient transport, which ultimately leads to tissue hypoxia and cell death. Previous experimental and modeling studies (5, 6, 8) have shown that tissue oxygenation patterns are significantly different in irradiated normal tissue compared to age-matched controls, and the differences are apparent as early as 3 days postirradiation; however, oxygen delivery to irradiated tissue recovers within 6 months postirradiation.

Radiation has been shown to up-regulate the inflammatory cascade (9–13), resulting in increased expression of several cell adhesion molecules (13, 14) and increased leukocyte-endothelial interaction (15) and permeability of the blood-brain barrier (16, 17). Treatment with anti-inflammatory agents [dexamethasone, monoclonal antibody (mAb) to cytokines, mAb to various adhesion molecules, etc.] may significantly attenuate the inflammatory response of irradiated brain tissue by inhibiting the expression of ICAM1 (ICAM-1) and several other adhesion molecules (10, 13, 14, 16).

The tissue response to ionizing radiation is not limited to tissue irradiated directly but can be demonstrated in neighboring populations (18). Radiation-induced bystander or abscopal effects are defined by the presence of the biological effects of radiation in cells and/or tissues that were not themselves in the field of irradiation. Although the bystander phenomenon *in vitro* has been well described over the past decade (19), out-of-field the radiation effect on tissue vasculature and oxygenation remains unclear. Animal studies have shown that all the cells in the liver are at the same risk of radiation-induced chromosome damage even if only a small fraction of the total liver is irradiated (19). In cases of partial-organ radiation exposure, for example, when the lung base was irradiated, there was marked chromosomal damage in the shielded lung apex (20). Out-of-field radiation pneumonitis in patients with small cell lung cancer treated with thoracic radiation has also been reported (21). In the brain, clinically late neuropsychological complications in patients who received focal radiotherapy for certain brain tumors have been shown in several studies. For example, cancer patients focally irradiated in the pitu-

¹ Address for correspondence: Department of Mechanical Engineering, Temple University, 1947 N. 12th St., Philadelphia, PA 19122; e-mail: mkiani@temple.edu.

itary hypothalamic area of the brain suffered damage in their memory region distal to the irradiated brain tissue (22). It is unclear whether up-regulation of inflammatory processes plays a role in these *in vivo* effects.

In this study, several indicators of oxygenation in normal tissue were studied in locally irradiated (single 20-Gy dose) mouse brain observed 6 and 24 h and 3, 7, 30, 60 and 120 days postirradiation. Fluorescence staining was used to visualize perfused vasculature and immunohistochemical staining was used to visualize anatomical vessels and to quantify tissue hypoxia. Unilaterally (one hemisphere) and bilaterally (both hemispheres) irradiated brains were compared to study the bystander effects of distal irradiation on normal tissue microvasculature. The effects of anti-TNFA (TNF- α) treatment on local and distal radiation-induced changes on brain tissue were also studied.

MATERIALS AND METHODS

Animals

Male (6–8-week-old) C57BL mice (Harlan Laboratories, Frederick, MD) were used to study the effect of ionizing radiation on brain vasculature at 3, 7, 30, 60 and 120 days postirradiation. All protocols were approved by the Animal Care and Use Committee of the University of Tennessee Health Science Center and followed the guidelines of the National Institutes of Health (NIH publication no. 85-23, revised in 1985).

Irradiation

The animals were anesthetized with an intraperitoneal (i.p.) injection of a mixture of 10 mg/kg xylazine and 87 mg/kg ketamine during the irradiation procedure. A single 20-Gy dose of irradiation was delivered using a 6 MV linear accelerator (Siemens Primus, Concord, CA). Radiation was delivered by using a 3.5-cm-diameter collimator in a single-field configuration, and a tissue-equivalent material was placed above the mouse's head to establish electronic equilibrium and ensure uniform delivery of the prescribed dose to the brain. The dose rate for all experiments was 3 Gy/min. In unilaterally irradiated brains, only one hemisphere of the brain (right side) was irradiated, while the other hemisphere was shielded. A thermoluminescence dosimeter (TLD, Keithley 36541) was used to measure the radiation dose outside the shielded area. The results indicated that the maximum out-of-field radiation dose at the edge of the collimator was less than 3.5% of the in-field dose.

Experimental Protocol

In this study a series of techniques adapted from the field of tumor biology was used to quantify vascularity, perfusion and hypoxia in normal tissue (23). Brains were examined at different times from both the irradiated and age-matched control groups (five animals for each group). Mice were sedated (as described above) and 0.3 ml of 10 mM EF5 [2-(2-nitro-1H-imidazol-1-yl)-N-(2, 2, 3, 3, 3-pentafluoropropyl) acetamide, National Cancer Institute] was injected retro-orbitally. Fifteen minutes later another 0.3 ml of EF5 (10 mM) was injected i.p. EF5, a pentafluorinated derivative of etanidazole, and one of its highly specific antibodies, ELK3-51 (Department of Radiation Oncology, The University of Pennsylvania Health System), were used to quantify levels of tissue hypoxia (23–26). Six hours after the initial EF5 injection, and to identify perfused vessels, a fluorescent dye (DiOC₇; 3,3-dihexyloxycarbocyanine, Molecular Probes) was injected retro-orbitally (1.0 mg/kg in 75% dimethyl sulfoxide) 1 min before the brain was removed and rapidly frozen (total time <1 min) and stored at –80°C. This dose of DiOC₇ has been shown to provide optimal visualization of perfused vasculature by preferentially

staining cells immediately adjacent to perfused vessels (20, 27). Brains were sectioned (10 μ m thick) at –20°C using a cryostat (Leica CM3050 S). Sections were mounted on poly-L-lysine-coated glass slides for later staining and imaging.

CD31 (Platelet endothelial adhesion molecule-1, BD Biosciences)/AEC (3-amino-9-ethylcarbazole, DAKO) staining was used to visualize the cerebral vessels in the cortical area of the frontal lobe (27). Vessels visualized using CD31 staining will be termed “anatomical vessels” to distinguish them from vessels visible after DiOC₇ staining (perfused vessels). On day 1 of analysis, slides were imaged for DiOC₇ (450 nm/520 nm) to map the location of perfused vessels. After DiOC₇ imaging, slides were fixed in cold (–10°C) acetone for 5 min in a Coplin jar, then air-dried for 5 min. Slides were then washed three times in calcium-free phosphate-buffered saline (PBS) and 5% normal mouse serum (Jackson ImmunoResearch) in buffer (PBS) at room temperature. Slides were then washed three times in PBS and once in Dako Peroxidase Blocking Reagent at room temperature, followed by three more washes in PBS. Finally, slides were incubated with 100 μ l rat anti-mouse CD31 antibody overnight (PharMingen, 1:10 dilution in Dako's Background Reducing Agent) at 4°C. On day 2, after slides were thawed for 30 min at room temperature, they were washed three times with PBS at room temperature and were then incubated with 100 μ l peroxidase-conjugated AffiniPure Mouse Anti-Rat IgG (H+L) at 1:25 dilution in Dako's Background Reducing Agent (40 μ g/ml) for 1 h at room temperature. Slides were then washed three times with PBS, incubated with 100 μ l of 5% normal mouse serum in buffer for 30 min at room temperature, washed with PBS, and incubated with 100 μ l ELK3.51-Cy3 (75 μ g/ml) overnight at 4°C. Tissue sections treated with the secondary antibody were used as negative controls. On day 3, slides were washed with PBS + Polyoxy ethylenesorbitan monolaurate (Tween 20, Sigma) and PBS.

Imaging Equipment and Procedures

Stained sections were imaged using an epi-fluorescence inverted TE200 Nikon microscope equipped with a motorized stage (model no. 99S008, LEP Ltd.) controlled by a computer using ImagePro (Media Cybernetics, Inc.). This computerized microscope system was used to obtain matching images for the same tissue after different staining procedures. Each section was scanned under three different staining conditions: Epi-illumination images of the fluorescent DiOC₇ staining were obtained immediately after 10- μ m sections were prepared. On day 3, after the completion of immunohistochemical staining procedures, the same brain section used for DiOC₇ imaging was rescanned under epi-illumination, and matching fluorescent red-orange montages were obtained showing the distribution of EF5/Cy3 staining, which is indicative of hypoxia; using transmitted light (100 W halogen), matching brownish-red montages of the staining were acquired.

In this system, the X-Y spatial coordinates for imaging DiOC₇-stained vessels were recorded automatically onto a computer. After the first scan, the X-Y spatial coordinates recorded were used to return to these specific positions (with a spatial repeatability of less than 2 μ m) to acquire the matched EF5/Cy3 and CD31/AEC images. The intensity values of EF5 images were recorded in each field to quantify the corresponding CD31 and DiOC₇ images. These images were then superimposed over the corresponding CD31- and DiOC₇-stained images to quantify the relationship between hypoxia and anatomical and perfused vascular configurations, respectively.

All fluorescent images of EF5 were obtained before the use of transmitted light (used for imaging of CD31 staining) to prevent fading of the EF5 stain. The resulting images from CD31 staining were enhanced using ImagePro to identify AEC-stained blood vessels. Similarly, DiOC₇-stained images were enhanced to determine the location of perfused vessels. The distribution of oxygen diffusion distances was determined as the measured distance from every point in the tissue to the nearest perfused blood vessel.

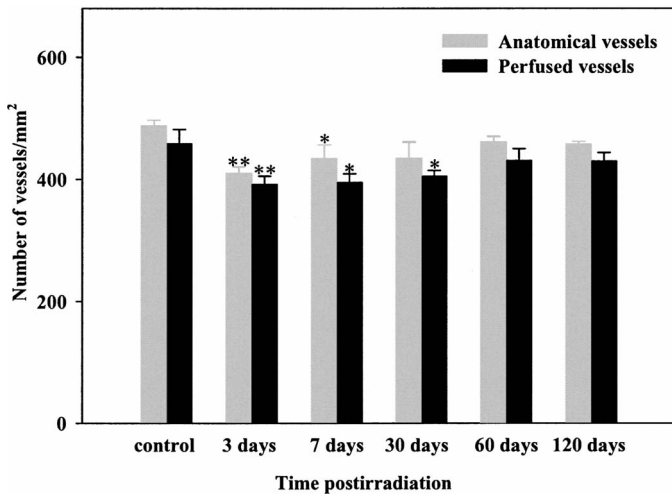


FIG. 1. In bilaterally (both hemispheres) irradiated brains, the number of anatomical and perfused vessels decreases up to 30 days postirradiation but returns to normal levels at later times (* $P < 0.05$ and ** $P < 0.01$ compared to age-matched control).

Anti-TNFA Treatment

Anti-TNFA mAb (clone MP6-XT3, BD Pharmingen) was injected retro-orbitally 15 min prior to irradiation. One hour before the animals were killed, they received another retro-orbital injection of anti-TNFA. Each injection contained 100 μ g of anti-TNFA mAb diluted in 0.1 ml of PBS.

Statistical Analysis

One-way ANOVA was used to determine significant differences among experimental groups, and Dunnett's test was used to differentiate between the means. Kolmogorov-Smirnov test (StatGraphics Plus; Manugistics) was used to compare frequency distributions. All data are reported as means \pm SEM. All values of $P < 0.05$ were considered statistically significant.

RESULTS

Bilateral Irradiation of the Brain

Mouse brains from age-matched controls and at 3, 7, 30, 60 and 120 days postirradiation (both hemispheres irradiated) were processed to quantify the density of anatomical and perfused vessels and levels of hypoxia. Compared to age-matched controls, at days 3, 7 and 30 postirradiation there was a significant decrease ($P < 0.01$) in the number of anatomical vessels (as indicated by CD31/AEC staining) as well as perfused vessels (as indicated by DiOC₇ staining) in bilaterally (both cerebral hemispheres) irradiated brains (Fig. 1). A significant increase in tissue hypoxia (as estimated from increase in intensity of EF5/Cy3) was observed 3 days postirradiation (Fig. 2) that returned to normal levels 60 days postirradiation. Consistent with these observations, the distance in the tissue to the nearest perfused blood vessel increased significantly ($P < 0.05$) 3, 7 and 30 days postirradiation and returned to by normal 60 days postirradiation (Fig. 3). As shown in Fig. 3, 80% of the tissue was within 20 μ m of the nearest perfused vessel in nonirradiated tissue (age-matched control animals), while at 3

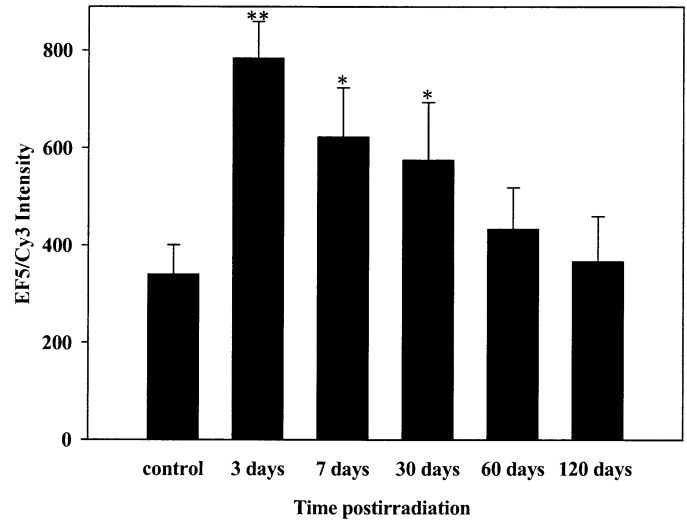


FIG. 2. In bilaterally (both hemispheres) irradiated brains, there is an increase in tissue hypoxia (as estimated from increase in the intensity of EF5/Cy3 staining) that peaks at 3 days postirradiation and returns to normal levels at later times (** $P < 0.01$ and * $P < 0.05$ compared to age-matched control).

days postirradiation about 30% of the tissue was within 20 μ m of the nearest perfused vessel. However, there was no significant change in vessel diameter in the irradiated compared to nonirradiated tissue (data not shown).

Unilateral Irradiation

Vascular density, levels of hypoxia, and oxygen diffusion distances were compared in irradiated and unirradiated cerebral hemispheres at different times. Right cerebral hemispheres of animals were irradiated with a single 20-Gy dose. Unilaterally irradiated brains were processed 6 and

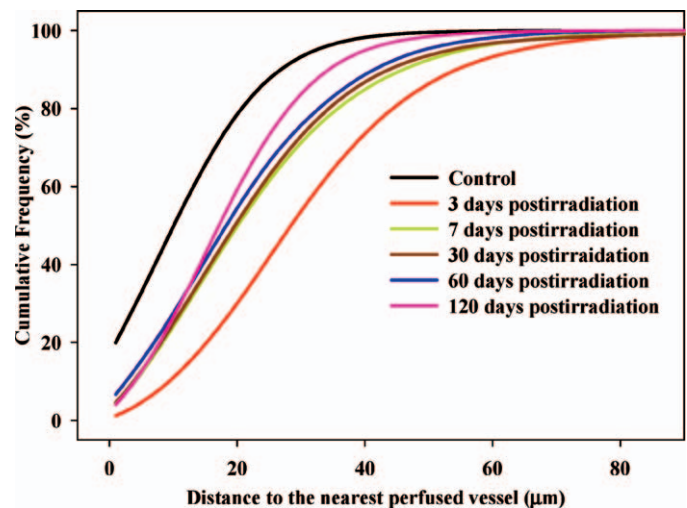


FIG. 3. In bilaterally (both hemispheres) irradiated brains, a decrease in the number of perfused vessels is accompanied by a significant ($P < 0.05$ compared to age-matched control) increase in the distance in the tissue to the nearest perfused vessel 3, 7 and 30 days postirradiation that returns to normal levels at later times.

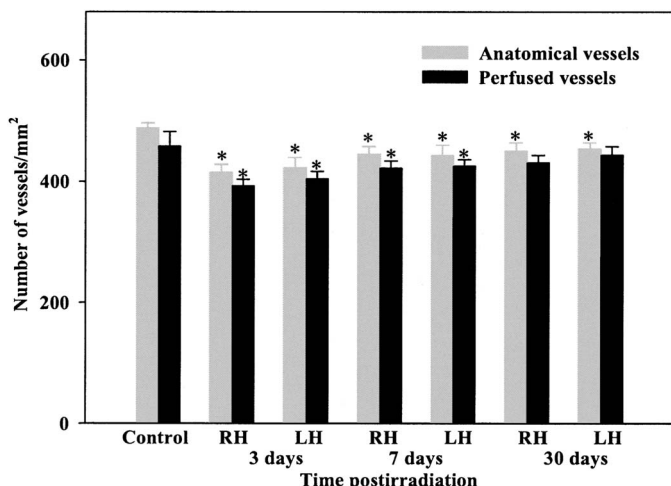


FIG. 4. As in the case of bilaterally irradiated animals (Fig. 1), in unilaterally (only right hemisphere) irradiated animals, the number of anatomical and perfused vessels decreases significantly in irradiated (RH, right hemisphere) as well as unirradiated (LH, left hemisphere) hemispheres (* $P < 0.05$ compared to control). The data for 6 and 24 h and 60 and 120 days postirradiation are not shown to simplify the graph.

24 h and 3, 7, 30, 60 and 120 days postirradiation to quantify the density of anatomical and perfused vessels and the levels of hypoxia in both irradiated (right side) and unirradiated (left side) cerebral hemispheres.

As shown in Figs. 4 and 5, in the unilaterally irradiated animals, both irradiated and unirradiated hemispheres of the brain showed similar significant changes compared to non-irradiated age-matched control animals in the numbers of anatomical and perfused vessels as well as the levels of hypoxia at each time. Changes in the distance to the nearest perfused vessel were also similar between irradiated and

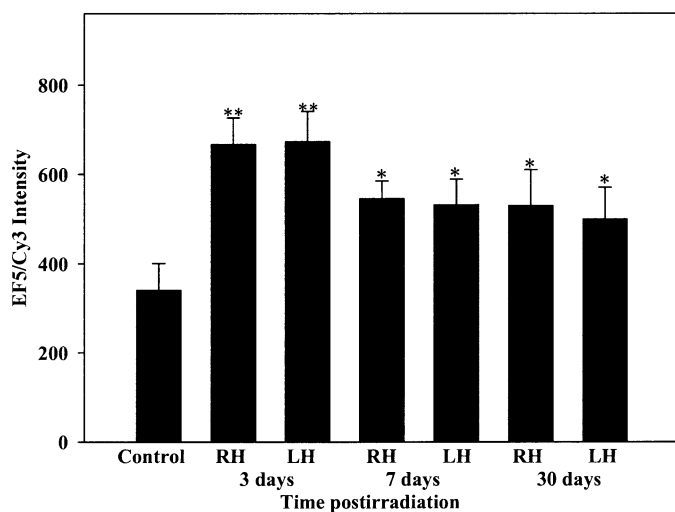


FIG. 5. As in the case of bilaterally irradiated animals (Fig. 2), in unilaterally irradiated brains (only right hemisphere), levels of hypoxia increase in irradiated (RH, right hemisphere) as well as unirradiated (LH, left hemisphere) hemispheres (** $P < 0.01$, * $P < 0.05$ compared to control). The data for 6 and 24 h and 60 and 120 days postirradiation are not shown to simplify the graph.

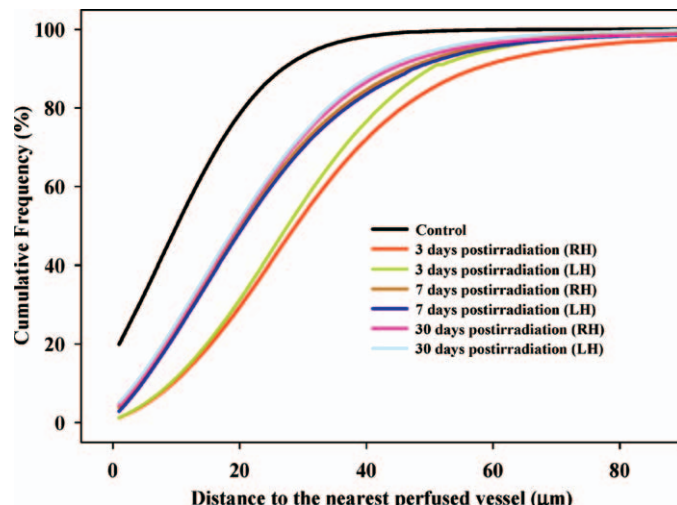


FIG. 6. As in the case of bilaterally irradiated animals (Fig. 3), in unilaterally (only right hemisphere) irradiated brains, a decrease in the number of perfused vessels is accompanied by a significant ($P < 0.05$ compared to control) increase in the distance in the tissue to the nearest perfused vessel in irradiated (RH, right hemisphere) as well as unirradiated (LH, left hemisphere) hemispheres. The data for 6 and 24 h and 60 and 120 days postirradiation are not shown to simplify the graph.

unirradiated hemispheres of unilaterally irradiated animals (Fig. 6).

Detectable changes in vascular density, oxygenation and oxygen diffusion distance in both hemispheres were significant as early as 24 h postirradiation (data not shown) and peaked at 3 days postirradiation. No significant differences between bilaterally and unilaterally irradiated brains were detected at any of the times.

Distal Organ Effect after Brain Irradiation

To determine if the abscopal effects could be detected in organs distal to the irradiated brain hemisphere, vascular density and tissue oxygenation were quantified using immunohistochemical staining in two distal organs (heart and lung). In the heart muscle, the numbers of anatomical and perfused vessels in animals 3 days postirradiation (unilaterally irradiated) were 512 ± 30 and 505 ± 43 vessels/mm², respectively, and were not significantly different from those of age-matched control (no brain irradiation) animals (549 ± 41 and 537 ± 37 , respectively). The average EF5/Cy3 intensity level (used as an index of hypoxia level) in heart muscle in irradiated animals was 305 ± 33 and was not significantly different from that of age-matched controls (262 ± 61). Similarly, hypoxia levels in lung tissue in irradiated animals (349 ± 53) were not significantly different from those of age-matched controls (320 ± 44). The numbers of anatomical and perfused vessels in the lungs could not be measured reliably using the immunohistochemical staining techniques outlined in this study.

Anti-TNFA Treatment Inhibits Radiation-Induced Effects

Previous studies have shown that TNFA and several cell adhesion molecules, including ICAM1, are up-regulated in

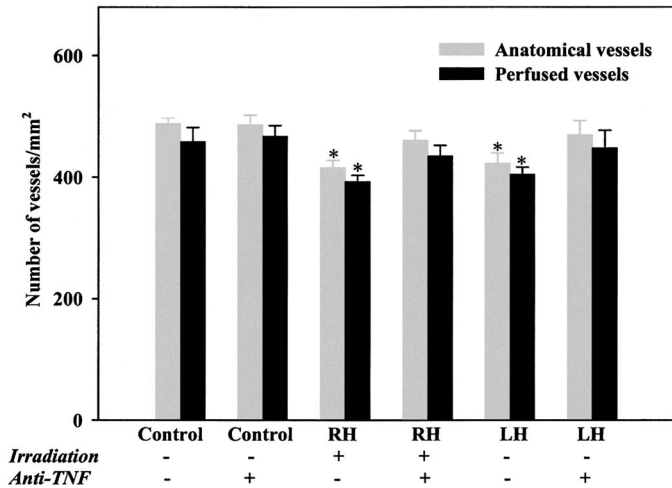


FIG. 7. Anti-TNFA treatment 3 days postirradiation inhibits radiation-induced decreases in the number of anatomical and perfused vessels in irradiated (RH, right hemisphere) as well as unirradiated (LH, left hemisphere) brain hemispheres (* $P < 0.05$ compared to control).

irradiated mouse brain and that mAb treatment can reduce the observed side effects of radiation exposure in the vasculature (10, 13, 14). As shown in Figs. 7 and 8, radiation-induced effects on the vascular density and the levels of hypoxia in both irradiated and unirradiated cerebral hemispheres were inhibited in animals treated with anti-TNFA mAb. These experiments were performed 3 days postirradiation, when radiation-induced changes in vascular density and oxygenation reached their peak. Consistent with these observations, there was no increase in the distance in the tissue to the nearest perfused blood vessel in anti-TNFA-treated animals (Fig. 9).

DISCUSSION

In this study, a novel series of techniques adapted from the field of tumor biology (28) were used to quantify vascularity, perfusion and levels of tissue hypoxia in the same sections of tissue after irradiation. The results indicate that the numbers of anatomical and perfused vessels, as well as levels of tissue hypoxia, are significantly different between irradiated (whole brain) and nonirradiated brains (age-matched control).

Furthermore, a single 20-Gy dose of ionizing radiation significantly alters the structure and function of microvascular networks not only in the irradiated brain hemisphere but also in the unirradiated hemisphere. However, treatment with anti-TNFA abrogates the observed changes in both irradiated and unirradiated cerebral hemispheres. In agreement with these findings, Kim *et al.* have shown that, compared to sham-irradiated animals, in a unilaterally irradiated (10 Gy) rat brain, there is a significant increase in TNFA expression in the irradiated as well as the unirradiated hemispheres (30).

The measured vascular density in normal and irradiated

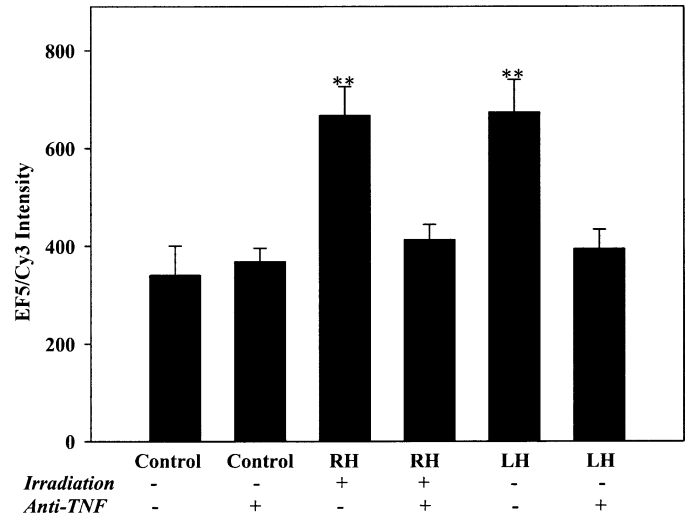


FIG. 8. Anti-TNFA treatment 3 days postirradiation inhibits radiation-induced hypoxia in brain tissue in irradiated (RH, right hemisphere) as well as unirradiated (LH, left hemisphere) brain hemispheres (** $P < 0.01$ compared to control).

brains in this study is in general agreement with that reported using similar techniques (31). In the present study, there was no significant difference in the number of anatomical/perfused vessels or in the levels of hypoxia between age-matched control groups in 6- and 36-week-old mice (data not shown).

To rule out the possibility that a small amount of out-of-field radiation may be responsible for the observed effects, a control study was performed in which both brain hemispheres were irradiated with 2 Gy; no change was observed in vascular density or levels of hypoxia (data not shown). Additionally, the levels of perfusion and hypoxia within unirradiated hemispheres did not correlate with distance from the edge of the radiation field (data not shown). To

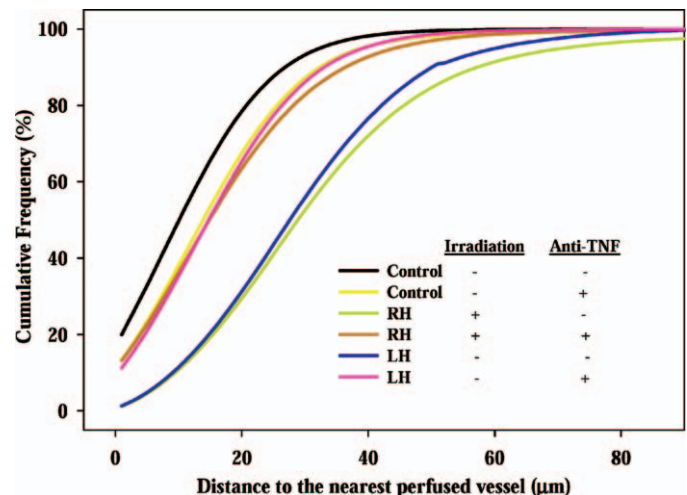


FIG. 9. At 3 days postirradiation, unilaterally irradiated (only right cerebral hemisphere, RH) animals treated with anti-TNFA show no significant difference in diffusion distances compared to unirradiated animals with or without anti-TNFA treatment ($P < 0.05$ compared to control).

determine if tissues more distal to the irradiated brain hemisphere are affected, vascular density and tissue oxygenation in the heart and lungs were measured using immunohistochemical staining. In this study, no significant differences were observed in vascular density and oxygen levels in heart and lung tissue between control animals and animals 3 days postirradiation (brain only with a single dose of 20 Gy).

Previous studies have shown that blocking cytokines and adhesion molecules can significantly modulate the up-regulation of the inflammatory cascade in irradiated animals (10, 13, 14, 16). In the present study, an anti-TNFA mAb was used to block the radiation-induced effects observed in the contralateral unirradiated mouse brain. Anti-TNFA is not small enough to cross the normal blood-brain barrier (BBB); however, the increased BBB permeability after irradiation may allow extravasation of this molecule (13). Radiation-induced increases in TNFA expression in the mouse brain may activate several signaling pathways, including MEK1/2, MAPK kinase3/6 (MKK3/6), and p38 kinase, which lead to *COX2* gene expression (14). Specific inhibitors of the various signaling pathways can be used to delineate specific signaling pathways involved in this phenomenon (32).

Studies by several groups (16, 33) have shown a transient increase in vascular permeability in the brain that returns to normal by 3 days postirradiation. A transient increase in brain interstitial volume may result in an apparent reduction in vascular density. However, the data presented here indicate that the decrease in vascular density and perfusion, along with the concomitant increase in tissue hypoxia, persists as late as 30 days postirradiation. Therefore, the transient increase in vascular permeability may explain the early changes in vascular density but not the later changes. Also, the observed increase in tissue hypoxia cannot be explained by a possible increase in vessel permeability. In addition to the observed increase in vascular permeability, a 15% decline in CNS endothelium within the first 24 h postirradiation (25–100 Gy) has also been shown (29). However, while in the latter study the decline in the number of endothelial cells continued at a slower rate at later times, we did not observe changes in vascular density beyond 30 days postirradiation.

In conclusion, the findings from this study indicate that radiation-induced vascular damage in mouse brain extends into the unirradiated hemisphere. Furthermore, these findings indicate that treatment with anti-TNFA abrogates the observed changes in the irradiated hemisphere as well as in the unirradiated hemisphere. Even though out-of-field radiation effects have been observed clinically, the clinical relevance of the vascular changes reported in this study to late CNS effects remains uncertain and requires further study. We are currently investigating the relationship between radiation-induced vascular changes and potential neural injury.

ACKNOWLEDGMENTS

This work was supported in part by grants from the DOD Breast Cancer Research Program and the Pennsylvania Department of Health. We thank Dr. Edmuth Chau for his assistance with dosimetry. Bin Wang is a predoctoral fellow of the American Heart Association. Mohammad F. Kiani is an Established Investigator of the American Heart Association.

Received: March 8, 2006; accepted: August 23, 2006

REFERENCES

1. L. F. Fajardo, The pathology of ionizing radiation as defined by morphologic patterns. *Acta Oncol.* **44**, 13–22 (2005).
2. L. A. Pena, Z. Fuks and R. N. Kolesnick, Radiation-induced apoptosis of endothelial cells in the murine central nervous system: Protection by fibroblast growth factor and sphingomyelinase deficiency. *Cancer Res.* **60**, 321–327 (2000).
3. F. Paris, Z. Fuks, A. Kang, P. Capodiceci, G. Juan, D. Ehleiter, A. Haimovitz-Friedman, C. Cordon-Cardo and R. Kolesnick, Endothelial apoptosis as the primary lesion initiating intestinal radiation damage in mice. *Science* **293**, 293–297 (2001).
4. H. B. Stone, W. H. McBride and C. N. Coleman, Modifying normal tissue damage postirradiation. Report of a workshop sponsored by the Radiation Research Program, National Cancer Institute, Bethesda, Maryland, September 6–8, 2000. *Radiat. Res.* **157**, 204–223 (2002).
5. N. M. Roth, M. R. Sontag and M. F. Kiani, Early effects of ionizing radiation on the microvascular networks in normal tissue. *Radiat. Res.* **151**, 270–277 (1999).
6. V. Nguyen, M. W. Gaber, M. R. Sontag and M. F. Kiani, Late effects of ionizing radiation on the microvascular networks in normal tissue. *Radiat. Res.* **154**, 531–536 (2000).
7. M. W. Gaber, M. D. Naimark and M. F. Kiani, Dysfunctional microvascular conducted response in irradiated normal tissue. *Adv. Exp. Med. Biol.* **510**, 391–395 (2003).
8. M. F. Kiani, R. Ansari and M. W. Gaber, Oxygen delivery in irradiated normal tissue. *J. Radiat. Res. (Tokyo)* **44**, 15–21 (2003).
9. M. H. Gaugler, C. Squiban, M. A. Van Der, J. M. Bertho, M. Vandamme and M. A. Mouthon, Late and persistent up-regulation of intercellular adhesion molecule-1 (ICAM-1) expression by ionizing radiation in human endothelial cells *in vitro*. *Int. J. Radiat. Biol.* **72**, 201–209 (1997).
10. M. F. Kiani, H. Yuan, X. Chen, L. Smith, M. W. Gaber and D. J. Goetz, Targeting microparticles to select tissue via radiation-induced upregulation of endothelial cell adhesion molecules. *Pharm. Res.* **19**, 1317–1322 (2002).
11. B. Prabhakarparandian, D. J. Goetz, R. A. Swerlick, X. Chen and M. F. Kiani, Expression and functional significance of adhesion molecules on cultured endothelial cells in response to ionizing radiation. *Microcirculation* **8**, 355–364 (2001).
12. S. Quarmby, P. Kumar and S. Kumar, Radiation-induced normal tissue injury: Role of adhesion molecules in leukocyte-endothelial cell interactions. *Int. J. Cancer* **82**, 385–395 (1999).
13. H. Yuan, D. J. Goetz, M. W. Gaber, A. C. Issekutz, T. E. Merchant and M. F. Kiani, Radiation-induced up-regulation of adhesion molecules in brain microvasculature and their modulation by dexamethasone. *Radiat. Res.* **163**, 544–551 (2005).
14. M. W. Gaber, O. M. Sabek, K. Fukatsu, H. G. Wilcox, M. F. Kiani and T. E. Merchant, Differences in ICAM-1 and TNF- α expression between large single fraction and fractionated irradiation in mouse brain. *Int. J. Radiat. Biol.* **79**, 359–366 (2003).
15. L. B. Johnson, A. A. Riaz, D. Adawi, L. Wittgren, S. Back, C. Thornberg, N. Osman, V. Gadaleanu, H. Thorlacius and B. Jeppsson, Radiation enteropathy and leukocyte-endothelial cell reactions in a refined small bowel model. *BMC Surg.* **4**, 10 (2004).
16. H. Yuan, M. W. Gaber, T. McColgan, M. D. Naimark, M. F. Kiani and T. E. Merchant, Radiation-induced permeability and leukocyte

- adhesion in the rat blood-brain barrier: Modulation with anti-ICAM-1 antibodies. *Brain Res.* **969**, 59–69 (2003).
17. H. Yuan, M. Gaber, K. Boyd, C. Wilson and M. M. Kiani, Effects of fractionated radiation on the brain vasculature in a mouse model: Blood-brain barrier permeability, cell adhesion, and ultrastructural changes. *Int. J. Radiat. Oncol. Biol. Phys.*, in press.
 18. A. Zhu, H. Zhou, C. Leloup, S. A. Marino, C. R. Geard, T. K. Hei and H. B. Lieberman, Differential impact of mouse Rad9 deletion on ionizing radiation-induced bystander effects. *Radiat. Res.* **164**, 655–661 (2005).
 19. W. F. Morgan, Non-targeted and delayed effects of exposure to ionizing radiation: II. Radiation-induced genomic instability and bystander effects *in vivo*, clastogenic factors and transgenerational effects. *Radiat. Res.* **159**, 581–596 (2003).
 20. M. A. Khan, R. P. Hill and D. J. Van, Partial volume rat lung irradiation: An evaluation of early DNA damage. *Int. J. Radiat. Oncol. Biol. Phys.* **40**, 467–476 (1998).
 21. J. Y. Wang, K. Y. Chen, J. T. Wang, J. H. Chen, J. W. Lin, H. C. Wang, L. N. Lee and P. C. Yang, Outcome and prognostic factors for patients with non-small-cell lung cancer and severe radiation pneumonitis. *Int. J. Radiat. Oncol. Biol. Phys.* **54**, 735–741 (2002).
 22. D. D. Roman and P. W. Sperduto, Neuropsychological effects of cranial radiation: Current knowledge and future directions. *Int. J. Radiat. Oncol. Biol. Phys.* **31**, 983–998 (1995).
 23. A. Maity, W. Sall, C. J. Koch, P. R. Oprysko and S. M. Evans, Low pO_2 and β -estradiol induce VEGF in MCF-7 and MCF-7-5C cells: Relationship to *in vivo* hypoxia. *Breast Cancer Res. Treat.* **67**, 51–60 (2001).
 24. E. M. Lord, L. Harwell and C. J. Koch, Detection of hypoxic cells by monoclonal antibody recognizing 2-nitroimidazole adducts. *Cancer Res.* **53**, 5721–5726 (1993).
 25. C. J. Koch, S. M. Evans and E. M. Lord, Oxygen dependence of cellular uptake of EF5 [2-(2-nitro-1H-imidazol-1-yl)-N-(2,2,3,3,3-pentafluoropropyl)acetamide]: Analysis of drug adducts by fluorescent antibodies vs bound radioactivity. *Br. J. Cancer* **72**, 869–874 (1995).
 26. S. M. Evans, K. D. Judy, I. Dunphy, W. T. Jenkins, W. T. Hwang, P. T. Nelson, R. A. Lustig, K. Jenkins, D. P. Magarelli and C. J. Koch, Hypoxia is important in the biology and aggression of human glial brain tumors. *Clin. Cancer Res.* **10**, 8177–8184 (2004).
 27. B. M. Fenton, S. F. Paoni, J. Lee, C. J. Koch and E. M. Lord, Quantification of tumour vasculature and hypoxia by immunohistochemical staining and HbO₂ saturation measurements. *Br. J. Cancer* **79**, 464–471 (1999).
 28. B. Wang, R. Ansari, Y. Sun, A. E. Postlethwaite, K. T. Weber and M. F. Kiani, The scar neovasculature after myocardial infarction in rats. *Am. J. Physiol. Heart Circ. Physiol.* **289**, H108–H113 (2005).
 29. N. V. Ljubimova, M. K. Levitman, E. D. Plotnikova and L. K. Eidus, Endothelial cell population dynamics in rat brain after local irradiation. *Br. J. Radiol.* **64**, 934–940 (1991).
 30. S. H. Kim, D. J. Lim, Y. G. Chung, T. H. Cho, S. J. Lim, W. J. Kim and J. K. Suh, Expression of TNF- α and TGF- β 1 in the rat brain after a single high-dose irradiation. *J. Korean Med. Sci.* **17**, 242–248 (2002).
 31. D. Paris, N. Patel, A. DelleDonne, A. Quadros, R. Smeed and M. Mullan, Impaired angiogenesis in a transgenic mouse model of cerebral amyloidosis. *Neurosci. Lett.* **366**, 80–85 (2004).
 32. H. Zhou, V. N. Ivanov, J. Gillespie, C. R. Geard, S. A. Amundson, D. J. Brenner, Z. Yu, H. B. Lieberman and T. K. Hei, Mechanism of radiation-induced bystander effect: Role of the cyclooxygenase-2 signaling pathway. *Proc. Natl. Acad. Sci. USA* **102**, 14641–14646 (2005).
 33. T. Siegal and M. R. Pfeffer, Radiation-induced changes in the profile of spinal cord serotonin, prostaglandin synthesis, and vascular permeability. *Int. J. Radiat. Oncol. Biol. Phys.* **31**, 57–64 (1995).